

Anisotropic Smoothing Using Double Orientations

Gabriele Steidl and Tanja Teuber

University of Mannheim, A5, 68131 Mannheim, Germany

steidl@math.uni-mannheim.de,
tteuber@kiwi.math.uni-mannheim.de
http://kiwi.math.uni-mannheim.de

Abstract. To improve the quality of image restoration methods directional information has recently been involved in the restoration process. In this paper, we propose a two step procedure for denoising images that is particularly suited to recover sharp vertices and X junctions in the presence of heavy noise. In the first step, we estimate the (smoothed) orientations of the image structures, where we find the double orientations at vertices and X junctions using a model of Aach et al. Based on shape preservation considerations this directional information is then applied to establish an energy functional which is minimized in the second step. We discuss the behavior of our new method in comparison with single direction approaches appearing, e.g., when using the classical structure tensor of Förstner and Gülch and demonstrate the very good performance of our method by numerical examples.

1 Introduction

Recently, much effort has been put into improving image restoration processes by involving directional information. Our paper contributes to this topic. We restrict our attention to the denoising of images $f \in L_2(\mathbb{R}^2)$ corrupted by heavy white Gaussian noise and the minimization of energy functionals

$$\arg \min_{u \in L_2} \left\{ \frac{1}{2} \|f - u\|_{L_2}^2 + \lambda J(u) \right\}, \quad (1)$$

where $J : L_2 \rightarrow \mathbb{R}_{\geq 0} \cup \{+\infty\}$ denotes a proper, convex, closed functional which is in addition positively homogeneous. Frequently applied examples of such functionals are

$$J(u) := \begin{cases} \int_{\mathbb{R}^2} \varphi(\nabla u) dx, & u \in \text{BV}_\varphi, \\ \infty, & u \in L_2 \setminus \text{BV}_\varphi, \end{cases} \quad (2)$$

where $\varphi(x) = \varphi_1(x) := |x_1| + |x_2|$ as in [1, 2] or $\varphi(x) = \varphi_2(x) := \sqrt{x_1^2 + x_2^2}$ as in the Rudin-Osher-Fatemi (ROF) model [3]. Here $\text{BV}_\varphi(\mathbb{R}^2) := \{u \in L_2(\mathbb{R}^2) : \int_{\mathbb{R}^2} \varphi(\nabla u) dx < \infty\}$ denotes the (anisotropic) space of functions of bounded variation equipped with the norm

$$\int_{\mathbb{R}^2} \varphi(\nabla u) dx := \sup_{\substack{V \in C_c^1(\mathbb{R}^2, \mathbb{R}^2) \\ V \in W_\varphi \text{ a.e.}}} - \int_{\mathbb{R}^2} u(x) \operatorname{div} V(x) dx, \quad (3)$$

where the *Wulff shape* $W_\varphi := \{x \in \mathbb{R}^2 : \langle x, y \rangle \leq \varphi(y) \forall y \in \mathbb{R}^2\}$ of φ is the unit square with horizontal and vertical edges in case $\varphi = \varphi_1$ and the unit circle for $\varphi = \varphi_2$. Note that other positively homogeneous, finite, convex, even functions φ with $\varphi(0) = 0$ and $\varphi(x) > 0$ for $x \neq 0$ can be used in (2) and that the spaces BV_φ are equivalent for all these functions [4]. Besides (2) we will also apply *inf convolution* functionals

$$J(u) := (J_1 \square J_2)(u) := \inf_{u=u_1+u_2} \{J_1(u_1) + J_2(u_2)\}, \quad (4)$$

where J_1, J_2 are nonnegative, proper, convex, closed and positively homogeneous. A possible choice for J_1 and J_2 suggested, e.g., in [5] are $\int_{\mathbb{R}^2} |\partial_x u_1| dx$ and $\int_{\mathbb{R}^2} |\partial_y u_2| dx$.

It is well known that for large regularization parameters λ model (2) with φ_1 and similarly the above inf convolution model tends to cut vertices vertically and horizontally while the ROF approach rounds them. Therefore we propose to introduce local directional information obtained from the double direction tensors of Aach et al. [6] into these functionals.

Outline of our paper. In Sec. 2 we recall the single orientation estimations provided by the structure tensor in [7]. Then we turn to the double orientation estimations proposed in [6], where we get some additional insights on the nullspaces of these tensors. In Sec. 3 we start with shape preservation facts as motivation for the subsequent introduction of our new directional denoising model. Furthermore, we discuss our orientation choice in comparison to the classical structure tensor. The good performance of our method is demonstrated by numerical examples in Sec. 4. Conclusions are given in Sec. 5. More details including proofs are contained in the accompanying preprint [8].

Related work. Image restoration by first approximating the local geometry and then involving it into the restoration process was suggested in various papers. A group of methods retrieves the local geometry by computing the Gülch/Förstner *structure tensor* and then uses its eigenvalues and orthogonal eigenvectors to define a *diffusion tensor* which steers the direction of the flux in PDEs. Tschumperlé [9] divided these methods into *divergence-based* [10], *trace-based* [11] and his *curvature-based* methods. The first approach is also related to the minimization of specific energy functionals, see, e.g., [12, 13]. The curvature-based method [14, 9] which is related to the *line integral convolution* [15] is better suited for the restoration of sharp edges than the other two methods, but our method is superior in the presence of heavy noise. Note that as in [16] the curvature-based method can include multiple directions. Various papers deal with the smoothing of normal vectors by minimizing certain energy functionals [17, 18, 19, 20, 21, 22] and use this information for subsequent denoising. In general these minimization procedures are much more expensive than our double direction approach. Kimmel, Sochen et al. suggested restoration techniques within the Beltrami framework [23]. The corresponding smoothing with the so-called 'short-time Beltrami kernel' differs from the bilateral filters [24] in the fact that it uses geodesic distances on the image manifold while the bilateral

kernel applies Euclidian distances. In [25], the authors considered special images containing rotated rectangle and established a unique functional both for finding the rotation angles and for denoising. However, the resulting algorithm is again a two step procedure. For a simpler two step approach we refer to [26]. So far, the best results behind our new method we have obtained by applying nonlocal means [27, 28]. An example is reported in Sec. 4.

2 Orientation Estimations

2.1 Single Orientation Estimations

Let $\Omega \subset \mathbb{R}^2$ be the image part of interest. For simplicity, we assume that $\Omega := B_\varepsilon(0)$ is the ball around 0 with radius ε . Our ideal assumption is that this part of the image corresponds to a function $f : \Omega \rightarrow \mathbb{R}$ which has constant values along a single direction r with $\|r\|_2 = 1$, i.e., $f = \varphi(s^\top \cdot)$ with $s := r^\perp = (r_2, -r_1)^\top$ and $\varphi : [-\varepsilon, \varepsilon] \rightarrow \mathbb{R}$. Then,

$$0 = \frac{\partial}{\partial r} f(x) = r^\top \nabla f(x) = r^\top \varphi'(s^\top x) s, \quad \forall x \in \Omega$$

holds true and we also have for a nonnegative weight function $w : \Omega \rightarrow \mathbb{R}$ that

$$0 = \int_{\Omega} w(x) (r^\top \nabla f(x))^2 dx = r^\top \int_{\Omega} w(x) \nabla f(x) \nabla f(x)^\top dx r. \quad (5)$$

If φ is not constant, then the symmetric, positive semidefinite matrix

$$\mathcal{J} := \int_{\Omega} w(x) \nabla f(x) \nabla f(x)^\top dx = \int_{\Omega} w(x) (\varphi'(s^\top x))^2 dx s s^\top$$

has rank one and r is an eigenvector of the eigenvalue 0. So far we have considered image parts with an ideal directional behavior. Since in applications we deal with noisy images, a pre-smoothing step with the 2D Gaussian K_σ of standard deviation σ is performed before computing the gradient in \mathcal{J} . Thus, (5) holds at least approximately and r is the minimizer of the weighted least squares expression $r^\top \mathcal{J} r$ subject to $\|r\|_2 = 1$, i.e., the eigenvector belonging to the smallest eigenvalue of \mathcal{J} . Moreover, in natural images the significant directions vary in different image parts. To detect the direction in the neighborhood of every image point x , we use the shifted Gaussian $w = K_\rho(\cdot - x)$ (truncated outside $B_{3\rho}(x)$). In this way, we can attach to each image point a 2×2 matrix, the so-called *structure tensor*

$$\mathcal{J}_\rho := K_\rho * (\nabla f_\sigma \nabla f_\sigma^\top), \quad \nabla f_\sigma := \nabla(K_\sigma * f).$$

If the eigenvalues of $\mathcal{J}_\rho(x)$ fulfill $\lambda_1 \ll \lambda_2$, then we are in the neighborhood of an edge and the orthogonal eigenvectors $r_1 = r$ and $r_2 = r^\perp$ approximate the *isophote direction* and the *gradient direction* in x . In the neighborhood of vertices, where $\lambda_2 \geq \lambda_1 \gg 0$, we obtain smoothed eigenvectors between neighboring edges. This causes artefacts in restoration models involving these directions. Therefore we are interested in double orientations.

2.2 Double Orientation Estimations

Assume that f can be decomposed into two functions $f_i = \varphi_i(s_i^T \cdot)$ with $s_i := r_i^\perp$, $i = 1, 2$, where $r_1 \not\parallel r_2$. As in Fig. 1, we consider two decompositions of f , the *transparent model*

$$f(x) = f_1(x) + f_2(x) \quad \forall x \in \Omega \tag{6}$$

and the *occlusion model* with $\Omega = \Omega_1 \cup \Omega_2$, $\Omega_1 \cap \Omega_2 = \emptyset$ and

$$f(x) = \begin{cases} f_1(x) & \text{for } x \in \Omega_1, \\ f_2(x) & \text{for } x \in \Omega_2. \end{cases} \tag{7}$$

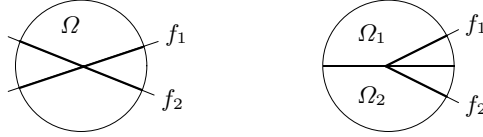


Fig. 1. Illustration of the transparent model (left) and the occlusion model (right)

Transparent model. By the definition of f_1 and f_2 we conclude for all $x \in \Omega$ that

$$0 = \frac{\partial^2}{\partial r_1 \partial r_2} f(x) = \frac{\partial^2}{\partial r_1 \partial r_2} (f_1(x) + f_2(x)) = r_2^T H(x) r_1 = r_1^T H(x) r_2 \tag{8}$$

with the *Hessian* $H(x)$ of f at x . Applying *tensor products* \otimes of matrices, (8) becomes

$$0 = (r_1 \otimes r_2)^T h(x) = (r_2 \otimes r_1)^T h(x) \quad \text{with } h := (\partial_{xx}f, \partial_{xy}f, \partial_{xy}f, \partial_{yy}f)^T \tag{9}$$

and since this holds true for all $x \in \Omega$ we also get

$$0 = \int_{\Omega} w(x) (r_1 \otimes r_2)^T h(x) h(x)^T (r_1 \otimes r_2) dx = (r_1 \otimes r_2)^T T (r_1 \otimes r_2) \tag{10}$$

with the symmetric, positive semidefinite matrix $T := \int_{\Omega} w(x) h(x) h(x)^T dx \in \mathbb{R}^{4,4}$. By (10) and since $r_1 \not\parallel r_2$, the vectors $r_1 \otimes r_2$ and $r_2 \otimes r_1$ are two linearly independent eigenvectors of the eigenvalue 0 of T . Instead of determining the directions r_1 and r_2 via (10), Aach et al. [6] proposed to rewrite (9) by skipping the double entry $\partial_{xy}f$ in h as

$$0 = r^T \tilde{h}(x) \quad \text{with } \tilde{h} := (\partial_{xx}f, \partial_{xy}f, \partial_{yy}f)^T, \quad r := (r_{11}r_{21}, r_{11}r_{22} + r_{12}r_{21}, r_{12}r_{22})^T. \tag{11}$$

Then our determining equation (10) becomes

$$0 = r^T \mathcal{T} r \quad \text{with } \mathcal{T} := \int_{\Omega} w(x) \tilde{h}(x) \tilde{h}(x)^T dx \in \mathbb{R}^{3,3} \tag{12}$$

and r is an eigenvector of 0 of the symmetric, positive semidefinite matrix \mathcal{T} . More precisely, we can prove that $\mathcal{T} = \mathcal{S} \Phi \mathcal{S}^T$ with $\mathcal{S} := (s_1 \otimes s_1, s_2 \otimes s_2)$, $v \otimes v := (v_1^2, v_1 v_2, v_2^2)^T$ and

$$\Phi := \int_{\Omega} w(x) \begin{pmatrix} (\varphi_1''(s_1^T x))^2 & \varphi_1''(s_1^T x) \varphi_2''(s_2^T x) \\ \varphi_1''(s_1^T x) \varphi_2''(s_2^T x) & (\varphi_2''(s_2^T x))^2 \end{pmatrix} dx$$

so that $rank \mathcal{T} = 0$ if $\varphi_i \in \Pi_1$, $i = 1, 2$, $rank \mathcal{T} = 1$ if $\varphi_i \in \Pi_1$ for exactly one i or $\varphi_i \in \Pi_2 \setminus \Pi_1$ for $i = 1, 2$, $rank \mathcal{T} = 2$ otherwise, where Π_n denotes the space of polynomials on $[-\varepsilon, \varepsilon]$ of degree $\leq n$. If $rank \mathcal{T} = 2$ (vertex case), then the nullspace of \mathcal{T} is $\mathcal{N}(\mathcal{T}) = \{c r : c \in \mathbb{R}\}$. If $rank \mathcal{T} = 1$ (edge case) and φ_1 is linear but φ_2 not, then $\mathcal{N}(\mathcal{T}) = \{(r_{11}c_1, r_{11}c_2 + r_{12}c_1, r_{12}c_2)^T : \mathbf{c} = (c_1, c_2)^T \in \mathbb{R}^2\}$, i.e., \mathbf{c} plays the role of r_2 in (11). There exist several possibilities to detect the directions r_i , $i = 1, 2$ from an eigenvector $u = (u_1, u_2, u_3)^T \in \mathcal{N}(\mathcal{T})$. For example, it is not hard to check that the following setting from [6] does the job: For $u_1 \neq 0$ set $r_1 := \frac{1}{\sqrt{u_1^2 + y_1^2}}(u_1, y_1)^T$, $r_2 := \frac{1}{\sqrt{u_1^2 + y_2^2}}(u_1, y_2)^T$, where y_i , $i = 1, 2$ are the solutions of the quadratic equation $y^2 - u_2 y + u_1 u_3 = 0$. If $u_1 = 0$, then $y_i = 0$ for one i and we set $r_i := \frac{1}{\sqrt{u_2^2 + u_3^2}}(u_2, u_3)^T$ and $r_{3-i} := (0, 1)^T$.

In the following, we choose as direction r_1 those fulfilling $|\langle r_1, \nabla f_{\tilde{\sigma}} \rangle| \leq |\langle r_2, \nabla f_{\tilde{\sigma}} \rangle|$. In particular, r_1 is the isophote direction at edges, where some vector \mathbf{c} plays the role of r_2 .

Oclusion model. By the definition of f_1 and f_2 we conclude for all $x \in \Omega$ that

$$0 = \frac{\partial}{\partial r_1} f(x) \frac{\partial}{\partial r_2} f(x) = (r_1^T \nabla f(x)) (r_2^T \nabla f(x)) = r_1^T \nabla f(x) \nabla f(x)^T r_2 \quad (13)$$

and by rewriting the equation using tensor products that

$$0 = (r_2 \otimes r_1)^T g(x) = (r_1 \otimes r_2)^T g(x) \text{ with } g := ((\partial_x f)^2, \partial_x f \partial_y f, \partial_x f \partial_y f, (\partial_y f)^2)^T.$$

This reads in the reduced form with r defined by (11) as

$$0 = r^T \tilde{g}(x) \text{ with } \tilde{g} := ((\partial_x f)^2, \partial_x f \partial_y f, (\partial_y f)^2)^T.$$

Since this relation is true for all $x \in \Omega$, we also have that

$$0 = r^T \mathcal{C} r \text{ with } \mathcal{C} := \int_{\Omega} w(x) \tilde{g}(x) \tilde{g}(x)^T dx. \quad (14)$$

Thus, r is an eigenvector of the eigenvalue 0 of the symmetric, positive semidefinite matrix \mathcal{C} . More precisely, we can prove that $\mathcal{C} = \alpha_1 (s_1 \otimes s_1)(s_1 \otimes s_1)^T + \alpha_2 (s_2 \otimes s_2)(s_2 \otimes s_2)^T$ with $\alpha_i := \int_{\Omega_i} w(x) (\varphi_i'(s_i^T x))^4 dx$, $i = 1, 2$, so that the rank of \mathcal{C} is $\nu \in \{0, 1, 2\}$ if exactly $2 - \nu$ of the functions φ_i are constant on Ω_i , $i = 1, 2$. The directions r_i , $i \in \{1, 2\}$ can be obtained from an eigenvector of $\mathcal{N}(\mathcal{C})$ as in the transparent model.

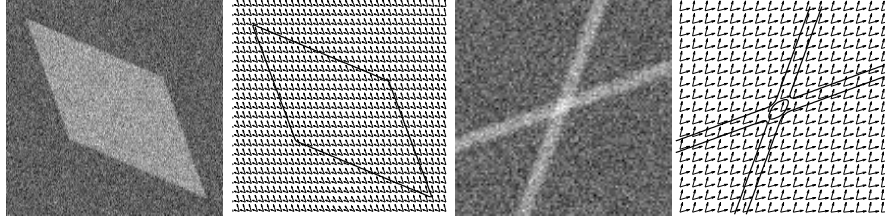


Fig. 2. Noisy images and their double orientation estimations by the occlusion model (left) and by the transparent model (right)

Double orientation tensors. In practice, we deal with noisy images having image parts with various significant directions. As for the classical structure tensor the *double orientation tensors* are defined as

$$\mathcal{T}_\rho := K_\rho * \left(\tilde{h}_\sigma \tilde{h}_\sigma^\top \right), \quad \mathcal{C}_\rho := K_\rho * \left(\tilde{g}_\sigma \tilde{g}_\sigma^\top \right),$$

where $\tilde{h} := (\partial_{xx}f_\sigma, \partial_{xy}f_\sigma, \partial_{yy}f_\sigma)^\top$, $\tilde{g} := ((\partial_x f_\sigma)^2, \partial_x f_\sigma \partial_y f_\sigma, (\partial_y f_\sigma)^2)^\top$ and the directions r_1, r_2 can be derived from an eigenvector of the smallest eigenvalue of $\mathcal{T}_\rho/\mathcal{C}_\rho(x)$. For an example of estimated double orientations see Fig. 2.

3 Image Restoration and Shape Preservation

We start with a proposition which characterizes the solution of (1).

Proposition 1. *The function $\hat{u} \in L_2$ is the solution of the minimization problem (1) iff* i) $\hat{u} = f - \lambda \hat{v}$, ii) $\hat{v} \in C_J := \{v \in L_2 : \langle v, w \rangle \leq J(w) \forall w \in L_2\}$,
iii) $\langle \hat{u}, \hat{v} \rangle = J(\hat{u})$.

For the special functional (2) we have that $\hat{v} \in C_J$ if there exists a vector field $\hat{V} \in L_\infty(\mathbb{R}^2, \mathbb{R}^2)$ such that $\hat{v} := -\text{div} \hat{V} \in L_2(\mathbb{R}^2)$ and $\hat{V} \in W_\varphi$ a.e. on \mathbb{R}^2 .

Using this proposition, one can prove that rectangles with horizontal and vertical edges [4] and + junctions [8] are preserved by the solution of (1) with (2) and $\varphi = \varphi_1$.

Corollary 1. *The solution \hat{u} of (1) with (2) and $\varphi = \varphi_1$ reads*

- i) for $f := c 1_\Omega$ with the characteristic function 1_Ω of $\Omega := (-a, a) \times (-b, b)$ as $\hat{u} = (c - \lambda \frac{a+b}{ab}) 1_\Omega$, $\lambda \leq \frac{cab}{a+b}$, $a, b > 0$,
- ii) for $f := c_1 1_{\Omega_1} + c_2 1_{\Omega_2}$ with $\Omega_1 := (-l, l) \times (-a, a)$, $\Omega_2 := (-b, b) \times (-l, l)$ as $\hat{u} = (c_1 - \lambda \frac{l+a}{la}) 1_{\Omega_1} + (c_2 - \lambda \frac{l+b}{lb}) 1_{\Omega_2}$, $\lambda \leq \min \left\{ \frac{c_1 la}{l+a}, \frac{c_2 lb}{l+b} \right\}$, $l > a, b > 0$.

In this paper, we propose to modify (2) (and similarly (4)) by locally including directions. The basic idea is that the minimizer of the modified functional also preserves shapes as, e.g., shown in Fig. 3 and arbitrary X junctions. This

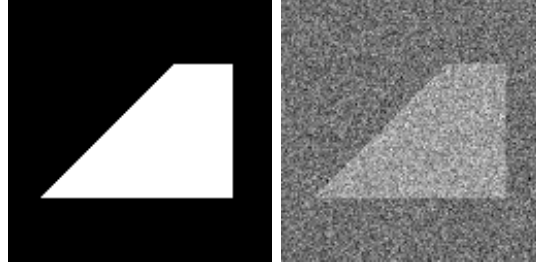


Fig. 3. Original and noisy trapezoid image (standard deviation 150)

modification can be motivated by the following considerations for a globally fixed transform matrix R : Substituting $x := R^{-1}t$, $f_R := f(R^{-1}\cdot)$, we obtain

$$\begin{aligned} & \frac{1}{2} \int_{\mathbb{R}^2} (f - u)^2 + \lambda \varphi(\nabla u) \, dx \\ &= \frac{1}{2|\det R|} \int_{\mathbb{R}^2} (f(R^{-1}t) - u(R^{-1}t))^2 + \lambda \varphi(\nabla_x u(R^{-1}t)) \, dt \\ &= \frac{1}{2|\det R|} \int_{\mathbb{R}^2} (f_R(t) - u_R(t))^2 + \lambda \varphi(R^T \nabla_t u_R(t)) \, dt. \end{aligned}$$

Whence, if \hat{u} minimizes the left-hand side, then the transformed image $\hat{u}_R := \hat{u}(R^{-1}\cdot)$ is a minimizer of

$$\frac{1}{2} \int_{\mathbb{R}^2} (f_R - u)^2 \, dx + \lambda \int_{\mathbb{R}^2} \varphi(R^T \nabla u) \, dx. \tag{15}$$

In the following, we consider **discrete square images** $\mathbf{f} := (f(x, y))_{x,y=0}^{n-1} \in \mathbb{R}^{n,n}$ in their columnwise reshaped form $f \in \mathbb{R}^N$, $N := n^2$. Instead of partial derivatives we use *forward differences* so that the discrete version of the gradient reads

$$D = \begin{pmatrix} D_x \\ D_y \end{pmatrix} := \begin{pmatrix} H_0 \otimes H_1 \\ H_1 \otimes H_0 \end{pmatrix}, \quad H_0 := \frac{1}{2} \begin{pmatrix} 1 & 1 & & \\ & 1 & 1 & \\ & & \ddots & \\ & & & 1 & 1 \\ & & & & 2 \end{pmatrix}, \quad H_1 := \begin{pmatrix} -1 & 1 & & \\ & -1 & 1 & \\ & & \ddots & \\ & & & -1 & 1 \\ & & & & 0 \end{pmatrix}.$$

Then problem (1) becomes

$$\arg \min_{u \in \mathbb{R}^N} \{ \|f - u\|_2^2 + \lambda J(u) \} \tag{16}$$

and (2) with $\varphi = \varphi_1$ resp. (4) with $\int_{\mathbb{R}^2} |\partial_x u_1| \, dx$ and $\int_{\mathbb{R}^2} |\partial_y u_2| \, dx$ read as

$$J(u) := \|Du\|_1, \quad \text{resp.} \tag{17}$$

$$J(u) := \min_{u=u_1+u_2} \{ \|D_x u_1\|_1 + \|D_y u_2\|_1 \}. \tag{18}$$

The solution of (16) can be characterized as in the continuous setting:

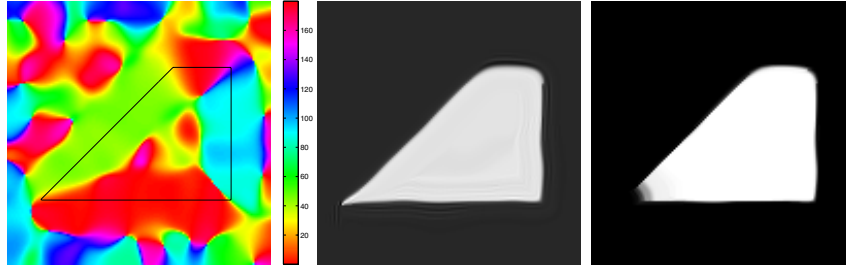


Fig. 4. Denoising with the directions r, r^\perp from the classical structure tensor. Left: Angle of $r \bmod 180^\circ$ ($\sigma = 2.5, \rho = 5$). The directions are smoothed near vertices following the *smallest way* between neighboring edge directions. Middle: Denoising result using only one direction $R := (r)$ ($\lambda = 2500$). Following this direction, obtuse vertices are rounded, while the acute one is prolonged. Right: Denoising result using both directions $R = (r_1, r_2) = (r, r^\perp)$ ($\lambda = 1000$). The edges of the minimizer \hat{u} tend to be aligned with one of the directions r_i , i.e., one of the summands $|\langle r_i, \nabla \hat{u} \rangle|, i = 1, 2$ becomes very small. Hence, rounding artefacts are visible at obtuse vertices, while the model decides for the wrong direction at the acute vertex which leads to a cut-off artefact.

Proposition 2. *The vector $\hat{u} \in \mathbb{R}^N$ is the solution of the minimization problem (16) if and only if i) - iii) of Proposition 1 hold true, where L_2 has to be replaced by \mathbb{R}^N with the Euclidian inner product. For the special functionals (17) and (18) we have that $\hat{v} \in C_J$ if and only if there exists a vector $\hat{V} = ((\hat{V}^{(1)})^T, (\hat{V}^{(2)})^T)^T \in \mathbb{R}^{2N}$ such that*

$$\begin{aligned} \hat{v} &:= D^T \hat{V} & \text{and} & \quad \|\hat{V}\|_\infty \leq 1, \quad \text{resp.}, \\ \hat{v} &:= D_x^T \hat{V}^{(1)} = D_y^T \hat{V}^{(2)} & \text{and} & \quad \|\hat{V}\|_\infty \leq 1. \end{aligned}$$

As in the continuous case rectangles and + junctions are preserved by the solution of (16) with (17). However, due to image boundaries one has to be careful with the discretization.

Corollary 2. *Let $x_0, y_0 \geq 0$ and $x_0 + a, y_0 + b \leq n - 2$. The solution \hat{u} of the minimization problem (16) with J defined by (17) reads for*

- i) $f := c 1_\Omega$ with $\Omega := \{x_0 + 1, \dots, x_0 + a\} \times \{y_0 + 1, \dots, y_0 + b\}$ as $\hat{u} = \left(c - \lambda \frac{2(a+b)}{ab}\right) 1_\Omega, \lambda \leq \frac{cab}{2(a+b)}$, where H_i are modified by $H_i(0,0) = 0, H_i(n-1, n-1) = (-1)^i, i = 0, 1$.
- ii) $f := c_1 1_{\Omega_1} + c_2 1_{\Omega_2}$ with $\Omega_1 := \{x_0 + 1, \dots, x_0 + a\} \times \{0, \dots, n-1\}, \Omega_2 := \{0, \dots, n-1\} \times \{y_0 + 1, \dots, y_0 + b\}$ as $\hat{u} = \left(c_1 - \lambda \frac{2}{a}\right) 1_{\Omega_1} + \left(c_2 - \lambda \frac{2}{b}\right) 1_{\Omega_2}, \lambda \leq \min\{\frac{ac_1}{2}, \frac{bc_2}{2}\}$, where H_i are modified by $H_0(n-1, 0) = 1, H_1(0,0) = 0, H_i(n-1, n-1) = (-1)^i, i = 0, 1$.

Similarly it can be shown that the inf convolution approach preserves + junctions [8].

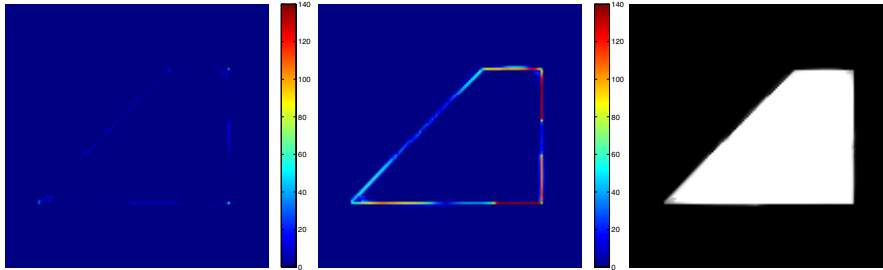


Fig. 5. Denoising with double orientations from the occlusion model. Left/Middle: Energies $|\langle r_i, \nabla \hat{u} \rangle|$, $i = 1, 2$. Except at isolated vertex points the model aligns the edges of the minimizer \hat{u} with the direction r_1 ($\sigma = 2$, $\rho = 9.5$). Right: Denoised image ($\lambda = 2500$). Although not perfect, this result is the best we got with various denoising methods so far.

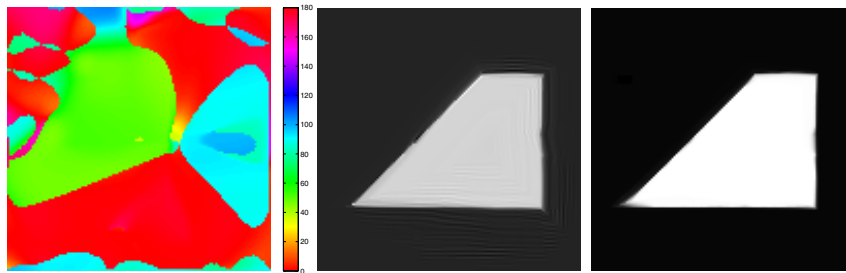


Fig. 6. Denoising with the single direction r_1 from the occlusion model. Left: Angle corresponding to the chosen direction ($\sigma = 2$, $\rho = 9.5$, $\tilde{\sigma} = 5\sigma$). Middle: Denoising with the regularization term $|\langle r_1, \nabla u \rangle|$ introduces textures at flat regions ($\lambda = 2500$). Right: Denoising with the regularization term $|\nabla u| - \langle r_1^\perp, \nabla u \rangle$ avoids these artefacts ($\lambda = 4500$).

Having (15) in mind we introduce our double orientations r_1, r_2 from Subsection 2.2 into (17) resp. (18) and consider for $\tilde{r}_i^\top = (\text{diag}(r_{i1}), \text{diag}(r_{i2}))$, $i = 1, 2$, the minimizers of our **new functionals**

$$\frac{1}{2} \|f - u\|_2^2 + \lambda \|\tilde{R}^\top Du\|_1 = \frac{1}{2} \|f - u\|_2^2 + \lambda (\|\tilde{r}_1^\top Du\|_1 + \|\tilde{r}_2^\top Du\|_1), \quad (19)$$

$$\frac{1}{2} \|f - u\|_2^2 + \lambda \min_{u=u_1+u_2} \{ \|\tilde{r}_1^\top Du_1\|_1 + \|\tilde{r}_2^\top Du_2\|_1 \}. \quad (20)$$

We want to examine the behavior of (19) by the simple denoising example in Fig. 3. First, we computed the minimizers using the directions r and r^\perp from the classical structure tensor. The appearing artefacts are commented in the caption of Fig. 4. Then, Fig. 5 shows the good denoising result with the proposed occlusion model for double orientations. Finally, Fig. 6 presents the denoising results

obtained by using only direction r_1 from this model. This leads to artefacts in flat regions, where the process introduces texture due to directional smoothing of heavy noise. This effect can be avoided by replacing $|\langle r_1, \nabla u \rangle|$ by $|\nabla u| - \langle r_1^\perp, \nabla u \rangle$. Note that we have to adapt the sign of r_1^\perp such that $\langle r_1^\perp, \nabla f_{\bar{\sigma}} \rangle \geq 0$ here. This functional was also proposed in [19] but with a more expansive procedure to find appropriate directions r_1^\perp .

4 Numerical Examples

In the following, we present further numerical examples. All programs were written in MATLAB, where we solved the minimization problems via their dual problem using second-order cone programming implemented in the software package MOSEK [29]. To discretize the derivatives occurring in the orientation estimation tensors we applied the filters suggested by Schar in [30]. The gray values of the original images are in $[0, 255]$ and for visualization we have used the MATLAB routine 'imagesc', which incorporates an affine gray value scaling. Moreover, the parameters are chosen with respect to the best visual result.

To start with, we took a noisy image with different shapes and restored it by nonlocal means, ROF and by (19) with occluding directions. The results are presented in Fig. 7. As already observed in [25] the result by ROF suffers from rounding artefacts at corners, since to remove all noise the regularization parameter λ has to be chosen rather large. This is avoided by (19) using occluding directions as visible at bottom right. The example with nonlocal means gives slightly worse results at corners. To demonstrate the performance on a real world image we included Fig. 8. Here, the example shows that the shape of

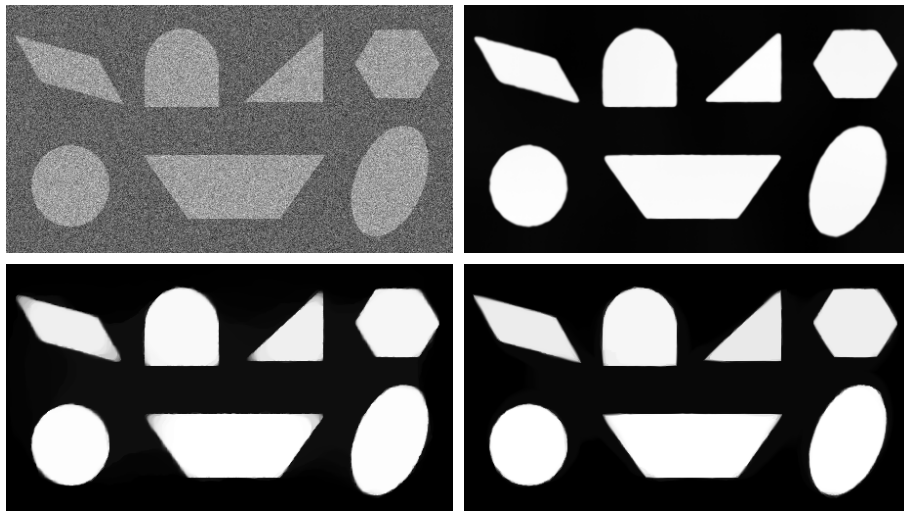


Fig. 7. Top: noisy image (standard deviation 100) and restored image by iterating two times the nonlocal means filter [28]. Bottom left: denoised image by ROF ($\lambda = 500$). Bottom right: restored image by (19) and occluding directions ($\lambda = 900$, $\sigma = 2$, $\rho = 6$).

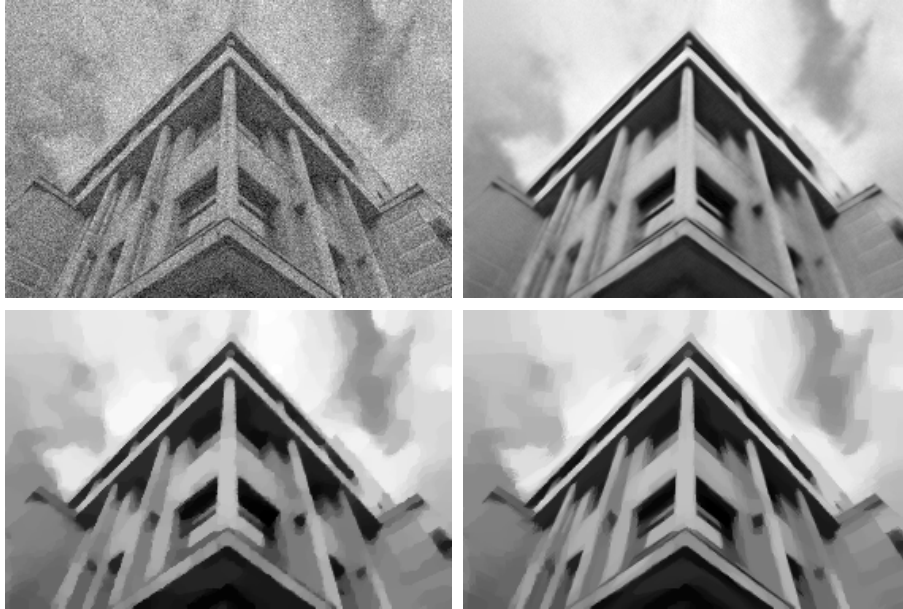


Fig. 8. Top: noisy image (standard deviation 30) and result by the nonlocal means filter [28]. Bottom left: denoised image by ROF ($\lambda = 50$). Bottom right: result by (19) and occluding directions ($\lambda = 50, \sigma = 0.5, \rho = 8$).

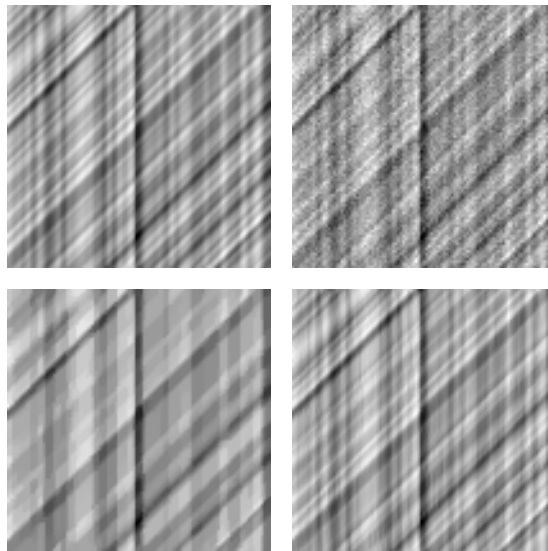


Fig. 9. Left to right: original image [30], noisy image (standard deviation 10), denoised image by (19) ($\lambda = 15, \sigma = 2, \rho = 12$), denoised image by (20) ($\lambda = 40, \sigma = 2, \rho = 12$). The directions are estimated by the transparent model.

the building is much better preserved by (19) than by ROF, since the local directions in the image are treated much more accurate. In contrast to nonlocal means, our method as well as ROF suffer from staircaising effects. However, for a large smoothing parameter related to the noise level nonlocal means creates small blur artefacts where our result has sharp structures. Besides, our method is computationally much faster. Finally, to point out the benefits of inf convolution, Fig. 9 shows restored images of an oriented texture by (19) and (20) resp. using the transparent model. For such images inf convolution is better suited than (19), since (19), like ROF, aims for a piecewise constant solution, which means that too many details are removed.

5 Conclusions

We have demonstrated how directional information estimated by the transparent or the occlusion model [6] can be integrated into certain minimization problems to improve the restoration results especially at sharp corners and X junctions. For simplicity we have restricted our attention to double orientations, but a generalization to more than two directions is possible with the results presented in [31]. To further improve the restoration results one option would be to use also higher order derivatives as done in [32]. Through this, it is for example possible to overcome the staircaising effects observed for (19).

References

1. Chambolle, A.: Total variation minimization and a class of binary MRF models. In: Rangarajan, A., Vemuri, B.C., Yuille, A.L. (eds.) EMMCVPR 2005. LNCS, vol. 3757, pp. 136–152. Springer, Heidelberg (2005)
2. Hintermüller, M., Kunisch, K.: Total bounded variation regularization as a bilaterally constrained optimization problem. *SIAM J. Appl. Math.* 4(64), 1311–1333 (2004)
3. Rudin, L.I., Osher, S., Fatemi, E.: Nonlinear total variation based noise removal algorithms. *Physica D* 60, 259–268 (1992)
4. Esedoglu, S., Osher, S.: Decomposition of images by the anisotropic Rudin-Osher-Fatemi model. *Comm. Pure and Applied Mathematics* 57(12), 1609–1626 (2004)
5. Chambolle, A., Lions, P.L.: Image recovery via total variation minimization and related problems. *Numerische Mathematik* 76, 167–188 (1997)
6. Aach, T., Mota, C., Stuke, I., Mühlich, M., Barth, E.: Analysis of superimposed oriented patterns. *IEEE Trans. on Image Processing* 15(12), 3690–3700 (2006)
7. Förstner, W., Gülch, E.: A fast operator for detection and precise location of distinct points, corners and centres of circular features. In: *Proc. ISPRS Intercommission Conf. on Fast Processing of Photogrammetric Data*, pp. 281–305 (1987)
8. Teuber, T.: Anisotropic smoothing using double orientations. Preprint University of Mannheim (2009)
9. Tschumperlé, D.: Fast anisotropic smoothing of multivalued images using curvature preserving PDEs. *International Journal of Computer Vision* 68(1), 65–82 (2006)
10. Weickert, J.: *Anisotropic Diffusion in Image Processing*. Teubner, Stuttgart (1998)
11. Tschumperlé, D., Deriche, R.: Vector-valued image regularization with PSDs: A common framework for different applications. *IEEE Trans. on Pattern Analysis and Machine Intelligence* 27(4) (2005)

12. Aubert, G., Kornprobst, P.: *Mathematical Problems in Image Processing: Partial Differential Equations and the Calculus of Variations*. Applied Mathematical Sciences, vol. 147. Springer, New York (2002)
13. Steidl, G., Teuber, T.: Diffusion tensors for denoising sheared and rotated rectangles (submitted) (2008)
14. Tschumperlé, D.: The CImg library. C++ Template Image Processing Library, <http://cimg.sourceforge.net>
15. Cabral, B., Leedom, L.C.: Imaging vector fields using line integral convolution. In: SIGGRAPH 1993, Computer Graphics, vol. 27, pp. 263–272 (1993)
16. Weickert, J.: Anisotropic diffusion filters for image processing based quality control. In: Fasano, A., Primicerio, M. (eds.) Proc. Seventh European Conference on Mathematics in Industry, pp. 355–362. Teubner, Stuttgart (1994)
17. Goldfarb, D., Wen, Z., Yin, W.: A curvilinear search method for p -harmonic flows on spheres. *SIAM Journal on Imaging Sciences* 2(1), 84–109 (2009)
18. Kimmel, R., Sochen, N.: Orientation diffusion or how to comb a porcupine? *Journal of Visual Communication and Image Representation* 13(1-2), 238–248 (2002)
19. Lysaker, O., Osher, S., Tai, X.C.: Noise removal using smoothed normals and surface fitting. *IEEE Trans. on Image Processing* 13(10), 1345–1357 (2004)
20. Vese, L., Osher, S.: Numerical methods for p -harmonic flows and applications to image processing. *SIAM Journal on Numerical Analysis* 40(6), 2085–2104 (2002)
21. Yuan, J., Schnörr, C., Steidl, G.: Convex Hodge decomposition and regularization of image flows. *Journal of Mathematical Imaging and Vision* 33(2), 169–177 (2009)
22. Rahman, T., Tai, X.C., Osher, S.: A TV-Stokes denoising algorithm. In: Sgallari, F., Murli, A., Paragios, N. (eds.) *SSVM 2007*. LNCS, vol. 4485, pp. 473–483. Springer, Heidelberg (2007)
23. Spira, A., Kimmel, R., Sochen, N.: A short-time Beltrami kernel for smoothing images and manifolds. *IEEE Trans. on Image Processing* 16(6), 1628–1636 (2007)
24. Tomasi, C., Manduchi, R.: Bilateral filtering for gray and color images. In: Proc. Sixth Intern. Conf. on Computer Vision, pp. 839–846. Narosa Publishing House (1998)
25. Berkels, B., Burger, M., Droske, M., Nemitz, O., Rumpf, M.: Cartoon extraction based on anisotropic image classification. In: *Vision, Modeling, and Visualization Proceedings*, pp. 293–300 (2006)
26. Setzer, S., Steidl, G., Teuber, T.: Restoration of images with rotated shapes. *Numerical Algorithms* 48(1-3), 49–66 (2008)
27. Buades, A., Coll, B., Morel, J.M.: A non-local algorithm for image denoising. In: *IEEE Int. Conf. on Comp. Vision and Pattern Recognition.*, vol. 2, pp. 60–65 (2005)
28. Manjón, J.V., Buades, A.: NL means. MATLAB Software, <http://dmi.uib.es/~abuades/software.html>
29. The MOSEK Optimization Toolbox, <http://www.mosek.com>
30. Schar, H.: Diffusion-like reconstruction schemes from linear data models. In: Franke, K., Müller, K.-R., Nickolay, B., Schäfer, R. (eds.) *DAGM 2006*. LNCS, vol. 4174, pp. 51–60. Springer, Heidelberg (2006)
31. Mühlich, M., Aach, T.: A theory for multiple orientation estimation. In: Leonardis, A., Bischof, H., Pinz, A. (eds.) *ECCV 2006*. LNCS, vol. 3952, pp. 69–82. Springer, Heidelberg (2006)
32. Setzer, S., Steidl, G.: Variational methods with higher-order derivatives in image processing. In: Neamtu, M., Schumaker, L.L. (eds.) *Approximation Theory XII: San Antonio 2007*, pp. 360–385. Nashboro Press (2008)